A Comparison of T$_2$ Relaxation-Based MRI Stroke Timing Methods in Hyperacute Ischemic Stroke Patients: A Pilot Study

Bryony L McGarry[1], Robin A Damion[1] iD, Isabel Chew[1],
Michael J Knight[1], George WJ Harston[2], Davide Carone[2],
Peter Jezzard[2], Amith Sitaram[3], Keith W Muir[3], Philip Clatworthy[4]
and Risto A Kauppinen[5] iD

[1]School of Psychological Science, University of Bristol, Bristol, UK. [2]Acute Stroke Programme,
Radcliffe Department of Medicine, University of Oxford, Oxford, UK. [3]Institute of Neuroscience
and Psychology, Queen Elizabeth University Hospital, University of Glasgow, Glasgow, UK.
[4]Stroke Neurology, Southmead Hospital, North Bristol NHS Trust, Bristol, UK. [5]Faculty of
Engineering, University of Bristol, Bristol, UK.

ABSTRACT

BACKGROUND: T$_2$ relaxation-based magnetic resonance imaging (MRI) signals may provide onset time for acute ischemic strokes with an unknown onset. The ability of visual and quantitative MRI-based methods in a cohort of hyperacute ischemic stroke patients was studied.

METHODS: A total of 35 patients underwent 3T (3 Tesla) MRI (<9-hour symptom onset). Diffusion-weighted (DWI), apparent diffusion coefficient (ADC), T$_1$-weighted (T$_1$w), T$_2$-weighted (T$_2$w), and T$_2$ relaxation time (T$_2$) images were acquired. T$_2$-weighted fluid attenuation inversion recovery (FLAIR) images were acquired for 17 of these patients. Image intensity ratios of the average intensities in ischemic and non-ischemic reference regions were calculated for ADC, DWI, T$_2$w, T$_2$ relaxation, and FLAIR images, and optimal image intensity ratio cut-offs were determined. DWI and FLAIR images were assessed visually for DWI/FLAIR mismatch.

RESULTS: The T$_2$ relaxation time image intensity ratio was the only parameter with significant correlation with stroke duration ($r = 0.49$, $P = .003$), an area under the receiver operating characteristic curve (AUC = 0.77, $P < .0001$), and an optimal cut-off (T$_2$ ratio = 1.072) that accurately identified patients within the 4.5-hour thrombolysis treatment window with sensitivity of 0.74 and specificity of 0.74. In the patients with the additional FLAIR, areas under the precision-recall-gain curve (AUPRG) and F$_1$ scores showed that the T$_2$ relaxation time ratio (AUPRG = 0.60, F$_1$ = 0.73) performed considerably better than the FLAIR ratio (AUPRG = 0.39, F$_1$ = 0.57) and the visual DWI/FLAIR mismatch (F$_1$ = 0.25).

CONCLUSIONS: Quantitative T$_2$ relaxation time is the preferred MRI parameter in the assessment of patients with unknown onset for treatment stratification.

KEYWORDS: Ischemic stroke, unknown onset, T$_2$ relaxation, signal intensities, DWI/FLAIR mismatch

Introduction

Unknown time of symptom onset due to "wake-up stroke" or lack of witness is a common contraindication for reperfusion therapies for ischemic stroke.[1,2] Intra-arterial administration of thrombolytic agents is considered safe within 6 hours of onset but is not routine,[3] and patients with large vessel occlusion (LVO) can now be considered for mechanical thrombectomy if symptom onset was within the last 24 hours.[4,5] For the many patients without LVO, intravenous (IV) thrombolysis using recombinant tissue plasminogen activator (rtPA) is the only alternative.[5] Current guidelines dictate rtPA must be administered within 4.5 hours from symptom onset due to increased risk of hemorrhage after this time point.[5] Multiparametric

magnetic resonance imaging (MRI) reveals pathophysiological changes in the ischemic brain parenchyma, enabling diagnosis, insight into the extent of ongoing tissue damage, and inference of stroke duration.[6] MRI may, therefore, aid treatment stratification of ischemic stroke patients with unknown symptom onset time by identifying patients who (1) are likely to be within the 4.5-hour IV rtPA treatment window or (2) have sufficient viable tissue that would suggest they may benefit from reperfusion therapy regardless of onset time.[7,8] This study focused on imaging methods aimed at achieving (1).

MRI contrasts, including diffusion-weighted imaging (DWI) or the quantitative measure of diffusion, the apparent diffusion coefficient (ADC), are extremely sensitive to ischemia. Studies

using rodent models showed DWI signals increase and ADC values decrease sharply within minutes of ischemia onset at the same cerebral blood flow (CBF) threshold for catastrophic energy failure.[9,10] Regions with low ADC, therefore, reflect tissue undergoing cytotoxic edema and the associated cellular changes.[6,11] The wide dynamic range of ADC provides an excellent contrast to the non-ischemic brain, and so is useful for diagnosing ischemia and localizing affected brain tissue.[6,12] However, ADC values in patients remain consistently low for several days after the insult,[13] making it an unsuitable parameter for stroke timing. Preclinical studies have shown that the T_1 and T_2 relaxation times that contribute to the signal of weighted images typically acquired in the clinic, such as DWI, T_2-weighted (T_2w), and T_2w FLAIR (FLAIR), also change early during ischemia but, compared with ADC, changes are small.[6] T_1 and T_2 relaxation times have been shown to have linear time dependency in rat stroke models,[14,15] and for T_2, this has been translated to human stroke,[16-19] suggesting quantification of the T_2 relaxation time may be a suitable method for stroke timing.

The T_2 relaxation-based signal changes that occur in DWI and FLAIR images after stroke have also been exploited for stroke timing using visual[20-22] and quantitative methods.[23,24] For both approaches, if the signal in the ischemic region in the FLAIR image (identified by DWI or ADC) is deemed not to be hyperintense, it is likely that the patient is within the treatment window and thus eligible for rtPA. For the visual DWI/FLAIR mismatch approach, the presence of a "mismatch" where a lesion is visible on DWI but not FLAIR scans, indicates patient eligibility.[20-22] For the quantitative approach, the eligibility is determined by whether the ratio of image intensity values between ischemic and nonischemic reference regions is below a specific optimal cut-off.[23,24] This approach has been studied using image intensities from ADC, DWI, T_2w, FLAIR, and T_2 relaxation images in animal models of ischemia[25,26] and ischemic stroke patients,[19,23,24,27,28] but the overall performance of these parameters has not been directly compared in hyperacute stroke patients.

The recent results of the "WAKE-UP" stroke trial[29] in which patients with DWI/FLAIR mismatch treated with IV rtPA showed an 11.5% increased favorable outcome compared with placebo and have provided further impetus for investigating the clinical benefit and application of MRI for timing the ischemic stroke. Potential stroke timing methods must be able to successfully discriminate between patients within and beyond the 4.5-hour rtPA time window. High sensitivity is essential to identify as many patients as possible who are eligible for rtPA, and high specificity is also imperative to avoid potentially harmful treatment. In this pilot study, the performance of quantitative and visual MRI-based stroke timing methods derived from the same cohort of hyperacute ischemic stroke patients was compared. The focus was on image intensity ratios of ADC, DWI, T_2w, T_2 relaxation and FLAIR images, and the DWI/FLAIR mismatch.

Methods

Patients

Patients were recruited from North Bristol NHS Trust Frenchay and Southmead Hospitals (Bristol), Queen Elizabeth University Hospital (Glasgow), and University of Oxford Radcliffe Department of Medicine's Acute Vascular Imaging Centre (Oxford) (between 03/2014 and 08/2018). Time of witnessed symptom onset, National Institute Health Stroke Scale (NIHSS), and the attending physician's stroke classification according to the Oxford Community Stroke Project Classification[30] were recorded on admission. All stroke subtypes were considered for enrolment, including lacunar stroke (LACS), partial anterior stroke (PACS), posterior circulation stroke (POCS), and total anterior circulation stroke (TACS). Before enrolment, all patients received noncontrast computerized tomography (NCCT) scans and were treated according to the standard-of-care protocol, including administration of IV rtPA if eligible. Patients were not offered endovascular reperfusion therapy at any site.

Patients, or their legal representative, provided informed consent. Enrolled patients had MRI scans within 9 hours of symptom onset. Exclusion criteria after enrolment included withdrawal from involvement in the study after initial consent, early termination of scan due to claustrophobia, unclear diagnosis, uncertainty regarding symptom onset time, movement artefacts, error in scan protocol, no evident lesion on ADC images, evidence of bilateral stroke, bias field problems in weighted images, and presence of both periventricular and parenchymal white matter hyperintensities on T_2w images.

The study received ethical approval from the South West Frenchay Research Ethics Committee (ref 13/SW/0256), Scotland A REC (ref 16/SS/0223), and UK National Research Ethics Service committees (refs 12/SC/0292 and 13/SC/0362) for participants in Bristol, Oxford, and Glasgow, respectively. Ethical approval allowed patients to be in the scanner for up to 20 minutes at Bristol and up to 30 minutes at Oxford and Glasgow. Total scan time allowed included set up of the patient and localizers as well as the MRI protocol. The study was carried out in accordance with the Declaration of Helsinki.

MRI

All sites used a 3T (3 Tesla) MRI scanner with a 32-channel head coil (Bristol: Philips Achieva, Glasgow: Siemens Magnetom Prisma, Oxford: Siemens Magnetom Verio). The MRI protocol detailed in Table 1 included multi *b*-value diffusion for computation of DWI and ADC images, multi-echo T_2 for computation of T_2 relaxation and T_2w images, and 3D (3-dimensional) T_1w images for anatomical reference and registration. The approved scan time at Oxford and Glasgow enabled the acquisition of T_2w FLAIR as well.

Table 1. MRI acquisition parameters.

	SEQUENCE	TR (MS)	TE (MS)	RESOLUTION (MM³)			ACQUISITION TIME (MIN: S)
Multi-echo T$_2$							
Bristol	GRASE	3000	20, 40, 60, 80, 100	$0.6 \times 0.6 \times 2.3$	–	–	3:09
Glasgow	TSE	12 500	9.5, 66, 123	$1.7 \times 1.7 \times 2.0$	–	–	2:03
Oxford	TSE	12 000	7.7, 77, 177	$1.8 \times 1.7 \times 2.0$	–	–	1:50
					TI (MS)	FLIP ANGLE	
3D T$_1$w							
Bristol	FFE	6.84	3.18	$1.0 \times 1.0 \times 1.1$	–	8°	4.54
Glasgow	MP RAGE	2200	2.28	$0.9 \times 0.9 \times 0.9$	900	9°	5.07
Oxford	MP RAGE	1800	4.55	$1.5 \times 1.5 \times 1.0$	900	8°	2.06
T$_2$w FLAIR							
Glasgow	TSE	10 000	93	$0.9 \times 0.9 \times 5.0$	2500	150°	3.02
Oxford	TSE	9000	96	$1.9 \times 1.9 \times 2.0$	2500	150°	2.08
					B VALUE, S/MM² (MULTIPLICITY)	INDEPENDENT GRADIENT DIRECTIONS	
Diffusion							
Bristol	SE-EPI	3009	60.5	$1.2 \times 1.2 \times 4.4$	0(1), 1000(3)	3	0.37
Glasgow	SE-EPI	8000	90	$0.9 \times 0.9 \times 2.0$	0(3), 1000(20)	20	3.03
Oxford	SE-EPI	5300	91	$1.8 \times 1.8 \times 5.0$	0(1), 1000(1)	3	1.00

Abbreviations: GRASE, Gradient and Spin Echo; mm, millimeters; MP RAGE, 3D T$_1$w Magnetization Prepared Rapid Acquisition Gradient Echo; ms, milliseconds; s, seconds; SE-EPI, Spin-Echo Echo Planar Imaging; TE, time of echo; TR, time of repetition; TI, time of inversion; TSE, Turbo Spin Echo; T$_1$ FFE, radiofrequency spoiled incoherent gradient echo; T$_2$w FLAIR, slice-selective T$_2$w Fluid Attenuated Inversion Recovery.

Image processing and analysis

Image processing and analysis steps are illustrated in Figure 1 and described in detail below. These methods were developed and implemented by Knight et al[19] and Damion et al,[18] and programs used included MATLAB release 2016b (The MathWorks, Inc, Natick, MA), FSL (FMRIB, Oxford, UK), MANGO version 4.1 (Research Imaging Institute, UT Health Science Center, San Antonio, TX) and SPM12 (Wellcome Trust Centre for Neuroimaging).

Image computation. For diffusion data using 3 orthogonal diffusion-sensitizing gradients at a common b value, orientation independent ADC images were calculated using

$$\text{ADC} = \frac{-\ln\left(\frac{S_1 S_2 S_3}{S_0^3}\right)}{3b}, \qquad (1)$$

where S_0 is the signal without diffusion weighting, b is the b value, and S_1, S_2, and S_3 are the signal intensities at the 3 orthogonal directions.

For diffusion-weighted data with 20 independent diffusion-gradient directions ($b = 1000\,\text{mm}^2\,\text{s}^{-1}$) and 3 $b = 0$ images, ADC values were obtained from mean diffusivity maps, which were computed using FSL DTIFIT. Effective diffusion-weighted images were created for $b = 1000\,\text{mm}^2/\text{s}$ using the registered S_0 and ADC images via

$$\text{DWI} = S_0 e^{\left(-1000 \times ADC\right)}. \qquad (2)$$

Echo-summed T$_2$w images were computed by summing all echoes of the TE series, followed by bias correction using FSL FAST.[31] Calculation of T$_2$ relaxation images involved fitting a mono-exponential decay on a voxel-wise basis.

Image registration. To ensure correct alignment between voxels across all images and that the midline of the brain was consistently defined, for each patient, T$_1$w, ADC, DWI, T$_2$w, T$_2$ relaxation, and FLAIR images were brain extracted using FSL BET[32] and registered to the same space. This involved nonlinear registration of the ADC images to the T$_2$w image space using FSL FNIRT via the diffusion S_0 image and the echo
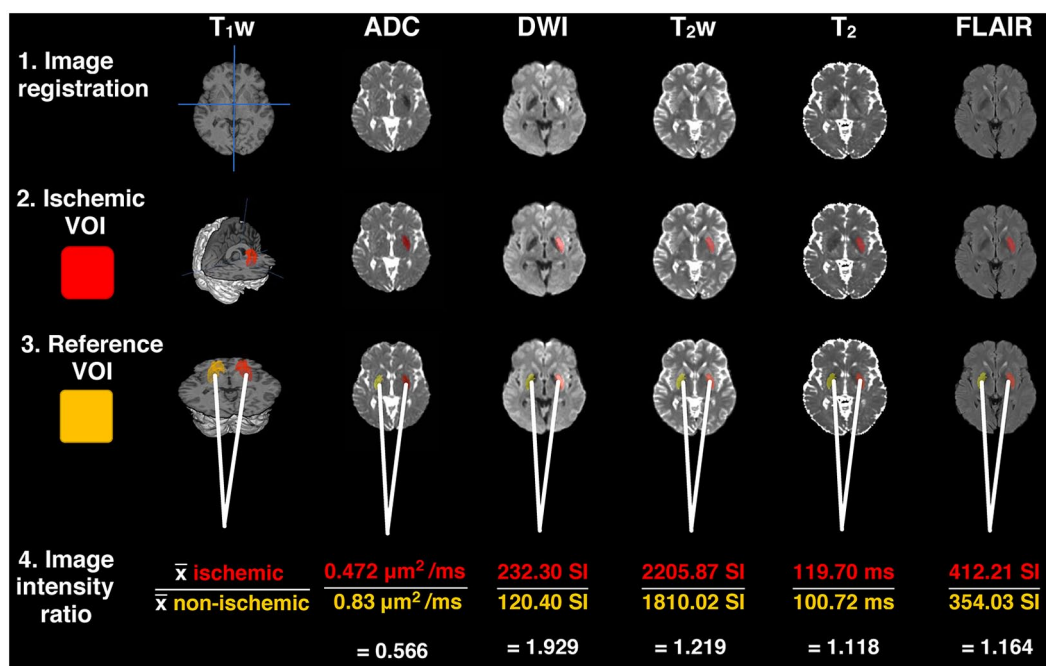
Figure 1. Summary of image processing and steps. (1) All images were registered to the same space. (2) ADC and T_2 limits defined the ischemic VOI. (3) Nonischemic reference VOIs were created by reflecting the ischemic VOI across the vertical axis, applying ADC and T_2 limits and manually editing if necessary. (4) Image intensity ratios were determined by dividing the average image intensity of the ischemic VOI by the average image intensity in the nonischemic VOI. Images shown are from the same patient (time from onset = 6 h 49 min, age = 59, thrombolysed before MRI, NIHSS = 13) and are representative of the image quality of scans acquired for all patients. ADC indicates apparent diffusion coefficient; VOI, volumes of interest.

summed T_2w image. If T_1w images were available, the T_2w image space was linearly registered (6 degrees of freedom) to the T_1w image space, which was subsequently registered to the MNI frame at $1 \, mm^3$ isotropic resolution using FSL FLIRT.[33] Where T_1w images were not available, the T_2w image space was, instead, directly registered (linearly) to the MNI frame at $1 \, mm^3$ isotropic resolution. All images were then linearly registered to the MNI frame using the registration maps (or combination of) generated by previous stages. The quality of co-registration across all image types was assessed visually by 2 independent assessors using SPM12 (BLM & IC). All images were deemed to be acceptably co-registered.

Lesion identification. The definition of ischemic voxels was those with ADC values >0.2-0.4 and <0.55-0.6 $\mu m^2/ms$ as well as ADC values less than one half-width half-maximum from the median ADC of nonischemic tissue. Limits of T_2 >30 and <200 ms were also applied to reduce the contribution from cerebral spinal fluid (CSF). These criteria were used to create lesion masks to define ischemic volumes of interest (VOIs). Refinement of ischemic VOIs involved removing all but the largest cluster (or clusters if there was more than 1 lesion). Selection of nonischemic reference VOIs required reflecting the ischemic VOI about the midline of axial slices (medial/lateral) applying the above T_2 limits and manually editing if CSF was visible within the VOI.

Computation of image intensity ratios. To approximate changes in image intensities due to ischemia, image intensity ratios

were calculated for each patient and image type, which involved dividing the mean value in the ischemic VOI by the mean value in the nonischemic reference VOI. Pre-ratio values were in milliseconds (ms) for T_2 relaxation images, $\mu m^2/ms$ for ADC, and signal intensities (SI, arbitrary units) for weighted images (DWI, T_2w, FLAIR). The purpose of computing ratios instead of using hemispheric differences in mean values was to reduce concerns that may arise from differences in pulse sequences, structures, and parameters between imaging sites.

Visual DWI/FLAIR mismatch. Four independent raters with experience in stroke MRI (RD, PC, AS, RAK) assessed DWI and FLAIR images. Raters were blinded to clinical details and asked to identify cases showing a "match" (visible hyperintensities in the same region on DWI and FLAIR), a "mismatch" (visible hyperintensity on DWI, not FLAIR), or cases they were uncertain about (no response). Raters viewed and applied thresholds to images according to personal preference. An arbitrator (KWM) with more than 25 years of experience in stroke MRI assessed images where there was uncertainty or disagreement between raters. Final classification as "match" or "mismatch" was based on majority classification, or KWM's adjudication when there was a 2-2 split in opinion.

Statistical analysis

Data from all 35 patients and the subcohort with the additional FLAIR scans were analyzed separately. This separation was to allow for a fair comparison of the performance of FLAIR with

other MRI classifiers. Statistical analysis was carried out using GraphPad Prism version 8.02 (GraphPad Software, La Jolla, CA), MedCalc Statistical Software version 19.0.5 (MedCalc Software bvba, Ostend, Belgium), and MATLAB release 2019a (The MathWorks, Inc, Natick, MA).

Data were assessed for normality using the Shapiro-Wilk test.[34] The difference between the average ADC values in the ischemic VOI between thrombolysed and non-thrombolysed patients was assessed using unpaired *t* tests. The relationships of image intensity ratios with time from symptom onset were assessed using Pearson correlations for normally distributed data and Spearman and Kendall correlations for non-normal data. Randolph free-marginal Fleiss Kappa calculator[35,36] was used to measure the agreement between the 4 DWI/FLAIR mismatch raters. All statistical tests were 2-tailed with a significance level of $P < .05$, and 95% confidence intervals (CIs) were calculated as $\pm 1.96 \times$ the standard error (SE) unless otherwise stated. The performance of MRI classifiers was compared using measures of accuracy (accuracy, sensitivity/recall, specificity), correctness (positive and negative predictive values), and probability (logistic regression). See ITEM 1 in the supplementary material for definitions and explanations of metrics used.

All patients. For a visual indication of the overall performance of MRI classifiers, receiver operating characteristic (ROC) curves were plotted. For a numerical indication of overall performance, areas under the ROC curves (AUC) were calculated and statistically compared using non-parametric methods that control for multiple comparisons.[37] Optimal image intensity ratio cut-offs were derived by the maximum Youden J Index, which identifies the cut-off that minimizes misclassification by giving equal weight to sensitivity and specificity.[38] Accuracy, sensitivity, specificity, positive predictive value (PPV), and negative predictive value (NPV) associated with these cut-offs were also calculated.

For further insight into the predictive performance of MRI classifiers, we also performed logistic regression analyses using MATLAB's Classification Learner app. Predictive generalized linear models were produced for individual image intensity ratios as well as a combination of all image intensity ratios. Predictive generalized linear models took the form of

$$Y = \alpha + \beta_1\chi_1 + \beta_2\chi_2 + \beta_3\chi_3 + \beta_4\chi_4 \cdots, \quad (3)$$

where Y is the predicted log odds of the patient being within the treatment window (Y = 1 for onset time < 270 minutes, Y = 0 for onset time > 270 minutes), α is the estimated intercept, $\beta_{1\ldots n}$ are the estimated regression coefficients, and $\chi_{1\ldots n}$ are the predictors (eg, image intensity ratio of ADC, DWI, T_2w, T_2).[36] The probability of being within the treatment window (*P*) could thus be calculated as

$$P = \frac{e^{(\alpha + \beta_1\chi_1 + \beta_2\chi_2 + \beta_3\chi_3 + \beta_4\chi_4 \cdots)}}{1 + e^{(\alpha + \beta_1\chi_1 + \beta_2\chi_2 + \beta_3\chi_3 + \beta_4\chi_4 \cdots)}}. \quad (4)$$

Equation (4) was used to generate probability plots for individual parameters providing a visual indication of the predictive power of models. The overall performance of the models was evaluated by comparing the significance of the χ^2 statistic and comparing the Akaike information criterion (AIC) values[37] corrected for sample size (AIC$_c$, see supplementary materials ITEM 1), where a low AIC$_c$ indicates a high-quality model.[39] For the combined model, the significance level of the *t*-statistic associated with each of the estimated coefficients (β) was used to assess the extent of the contribution of each parameter to the model.

Subcohort with FLAIR MRI. Different methods of evaluation were applied to the subcohort of patients with the additional FLAIR scans due to the imbalance in class sizes (n = 5 with onset times less than 4.5 hours, n = 12 with onset times greater than 4.5 hours). In data sets where there is a class imbalance, traditional ROC curves and AUCs are not recommended as they place more weight on the larger class and portray an overly optimistic view of overall performance.[40,41] Instead, in cases where there is low prevalence in the positive compared with the negative class (ie, 5 patients within the treatment window in this study), it has been recommended to use performance metrics such as precision/PPV and recall/sensitivity, which do not use the true negative contingency class in their definitions.[41-43] We, therefore, applied the precision-recall-gain (PRG) approach,[42] which performs well in class-imbalanced data sets while maintaining the benefits associated with ROC analysis (see ITEM 1 in supplementary material).

For a visual indication of the overall performance of MRI classifiers, precision-recall-gain (PRG) curves were plotted, and for a numerical indication, areas under the PRG curves (AUPRG) were calculated using open-source MATLAB software (see http://people.cs.bris.ac.uk/~flach/PRGcurves//). An AUPRG of 0 indicates a trivial (random) classifier, and positive and negative AUPRGs indicate more and less optimal classifiers, respectively. To compare the performance of image intensity ratios with the visual DWI/FLAIR mismatch, F_1 scores[44] were calculated for the DWI/FLAIR mismatch and image intensity ratio cut-offs. The F_1 score gives equal weighting to the importance of precision and recall and is considered an appropriate evaluation measure for imbalanced data sets.[45] For each parameter, the image intensity ratio with the highest F_1 score was chosen for comparison.

Results

Sixty-five patients were enrolled in the study. Thirty were not included in the final analysis due to bilateral stroke (n = 4) and the presence of both periventricular and parenchymal white matter hyperintensities (n = 2), no evidence for ischemia on ADC images (n = 11), uncertainty over stroke diagnosis (n = 3), movement artefacts (n = 1), ADC or T_2 not acquired (n = 4), vague onset time recorded (n = 3), MRI declined after consent (n = 1), and the early termination of scanning due to claustrophobia (n = 1).

Table 2. Clinical and imaging characteristics.

	ALL PATIENTS	SUBCOHORT WITH FLAIR
Patients, No. (%)	35	17
Female, No. (%)	13 (37.1)	3 (17.6)
Age, median (min-max)	68 (31-85)	67 (49-85)
NIHSS,[a] median (min-max)	8 (1-28)	8 (1-28)
Study site, No. (%)		
Bristol	17 (48.6)	0
Oxford	5 (14.3)	4 (23.5)
Glasgow	13 (37.1)	13 (75.5)
Stroke type,[b] No. (%)		
LACS	12 (34.3)	6 (35.3)
PACS	12 (34.3)	9 (52.9)
POCS	3 (8.6)	0
TACS	8 (22.9)	2 (11.8)
Left hemisphere, No. (%)	16 (45.7)	9 (52.9)
Thrombolysis		
Patients received rtPA, No. (%)	26 (74.3)	14 (82.4)
Median time from onset to rtPA, hours:mins (min-max)	2:05 (1:02-3:55)	2:32 (1:05-3:55)
Median time from rtPA to MRI, hours:mins (min-max)	3:37 (0:29-7:18)	4:20 (1:10-7:18)
Time from onset to MRI		
All patients, median hours:mins (min-max)	5:34 (2:25-9:29)	6:46 (2:28-9:29)
0-≤4.5 h		
Patients, No. (%)	16 (45.7)	5 (29.4)
Median hours:mins (min-max)	3:22 (2:25-4:25)	3:00 (2:28-3:10)
>4.5-≤9.5 h		
Patients, No. (%)	19 (54.3)	12 (70.6)
Median hours:mins (min-max)	6:55 (5:08-9:29)	6:59 (5:34-9:29)
VOI characteristics		
Median ADC lesion volume, mL (min-max)	1.99 (0.04-54.6)	5.50 (0.11-25.01)
Median ischemic ADC, $\mu m^2/ms$ (min-max)	0.53 (0.39-0.58)	0.51 (0.39-0.58)
Median nonischemic ADC, $\mu m^2/ms$ (min-max)	0.77 (0.36-1.00)	0.79 (0.69-0.89)

Abbreviations: ADC, apparent diffusion coefficient; LACS, lacunar; mL, milliliters; ms, milliseconds; MRI, magnetic resonance imaging; NIHSS, National Institutes of Health Stroke Scale; PACS, Partial Anterior Circulation; POCS, Posterior Circulation; rtPA, recombinant tissue plasminogen activator; TACS, Total Anterior Circulation; VOI, volume of interest.
[a]Scores on the NIHSS range from 0-42, higher scores indicate greater deficit.
[b]Strokes classified according to the Oxford Stroke Classification Scale.[30]

A summary of the clinical and imaging characteristics of all 35 patients and the subcohort with FLAIR scans is shown in Table 2. Total MRI acquisition times were 8 minutes, 14 minutes 9 seconds, and 7 minutes 9 seconds for Bristol, Glasgow, and Oxford, respectively. Results for Shapiro-Wilk tests, and Pearson, Spearman, and Kendall correlations are given in SI Table 1 in the supplementary materials document. Mean ADC values ($\mu m^2/ms$) in ischemic and non-ischemic reference VOIs
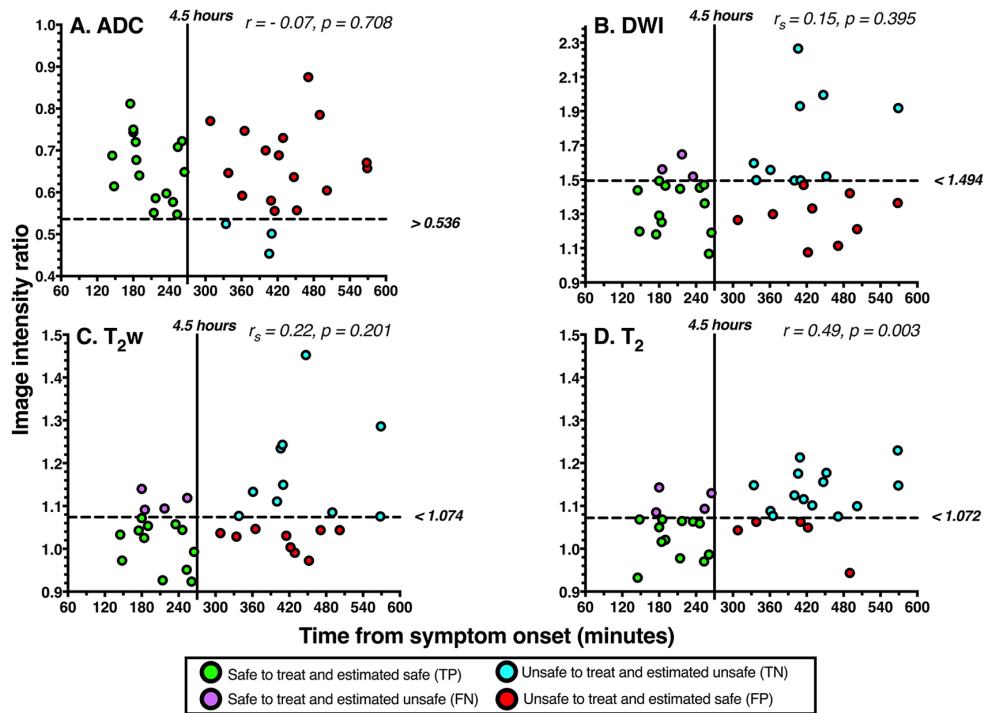
Figure 2. Relationship of image intensity ratios with time from symptom onset for (A) ADC, (B) DWI, (C) T_2w, and (D) the T_2 relaxation time. Correlation coefficients and *P* values are shown for each parameter. Pearson correlation coefficients (*r*) are shown for ADC and T_2 as they were normally distributed. Spearman rank correlation coefficients (r_s) are shown for DWI and T_2w as they were not normally distributed. Horizontal dashed lines represent optimal image intensity ratio cut-offs identified by the maximum Youden J index, which are labeled to the right of each figure. Vertical solid lines represent the 4.5-hour thrombolysis treatment-window cut-off. Data points represent individual patients and are color-coded according to the classification instructed by the optimal image intensity ratios. Green indicates a true positive case (TP), blue indicates a true negative case (TN), purple indicates a false negative case (FN), and red indicates a false positive case (FP). Data are from all 35 patients. ADC indicates apparent diffusion coefficient; DWI, diffusion-weighted imaging.

were consistent with previous reports in patients.[46] There was no difference between average ADC values in ischemic VOIs between thrombolysed and non-thrombolysed patients, for all 35 patients, thrombolysed: M = 0.50, SD = 0.05 vs non-thrombolysed: M = 0.54, SD = 0.05, *t*(33) = 2.02, *P* = .052, and the subcohort with FLAIR scans, thrombolysed: M = 0.49, SD = 0.06 vs non-thrombolysed: M = 0.54, SD = 0.02, *t*(15) = 1.35, *P* = .197.

All 35 patients. Figure 2 shows the T_2 relaxation time intensity ratio was the only parameter that correlated significantly with time from symptom onset (statistics given in SI Table 1 of supplementary materials).

The T_2 relaxation time image intensity ratio also showed the highest overall ability at distinguishing between patients scanned before and after 4.5 hours as the ROC curve was closer to the top left-hand corner of the ROC graph, and it was the only parameter with a significantly high AUC (Figure 3). There was no statistical difference between the AUCs of any of the parameters (see SI Table 2 in supplementary materials).

Figure 4 shows accuracy, sensitivity, and specificity values for optimal image intensity ratio cut-offs. As seen, the T_2 relaxation time ratio had the highest accuracy, and the sensitivity and specificity levels were high and comparable. For ADC, DWI, and T_2w, there was a trade-off, where most patients within the thrombolysis time window were correctly identified (high
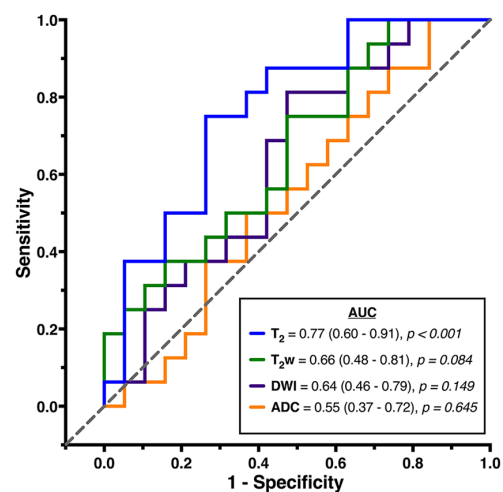

Figure 3. ROC curves showing the overall ability of image intensity ratios for distinguishing between ischemic stroke patients scanned before or after 4.5 hours from symptom onset. Lines closer to the grey dashed 0.5 reference line indicate parameters with poor overall ability. The closer the line to the top left-hand corner of the ROC graph, the higher the overall ability. AUC and *P* values are displayed for each MRI parameter with 95% binomial exact confidence intervals in brackets. An AUC with *P* > .05 indicates an AUC that does not significantly differ from an AUC of 0.5 and therefore performs no better than chance. Results are from all 35 patients. ADC indicates apparent diffusion coefficient; AUC, area under the curve; DWI, diffusion-weighted imaging; MRI, magnetic resonance imaging; ROC, receiver operating characteristic.
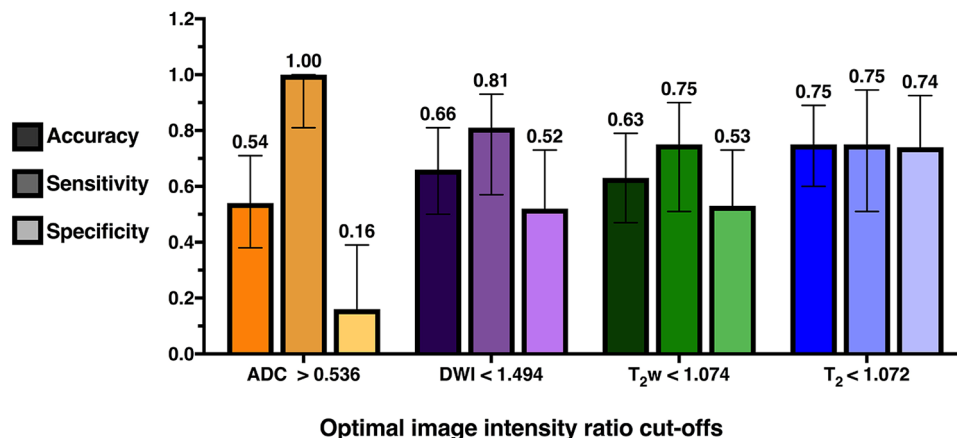
Figure 4. Accuracy, sensitivity, and specificity of optimal image intensity ratio cut-offs identified by the maximum Youden J index. For each parameter, the first darker shaded bar represents the accuracy, the second lighter shaded bar represents sensitivity, and the lightest third bar represents specificity. Corresponding values are labeled above the error bars, which represent the 95% confidence intervals. Results are from all 35 patients. ADC indicates apparent diffusion coefficient; DWI, diffusion-weighted imaging.
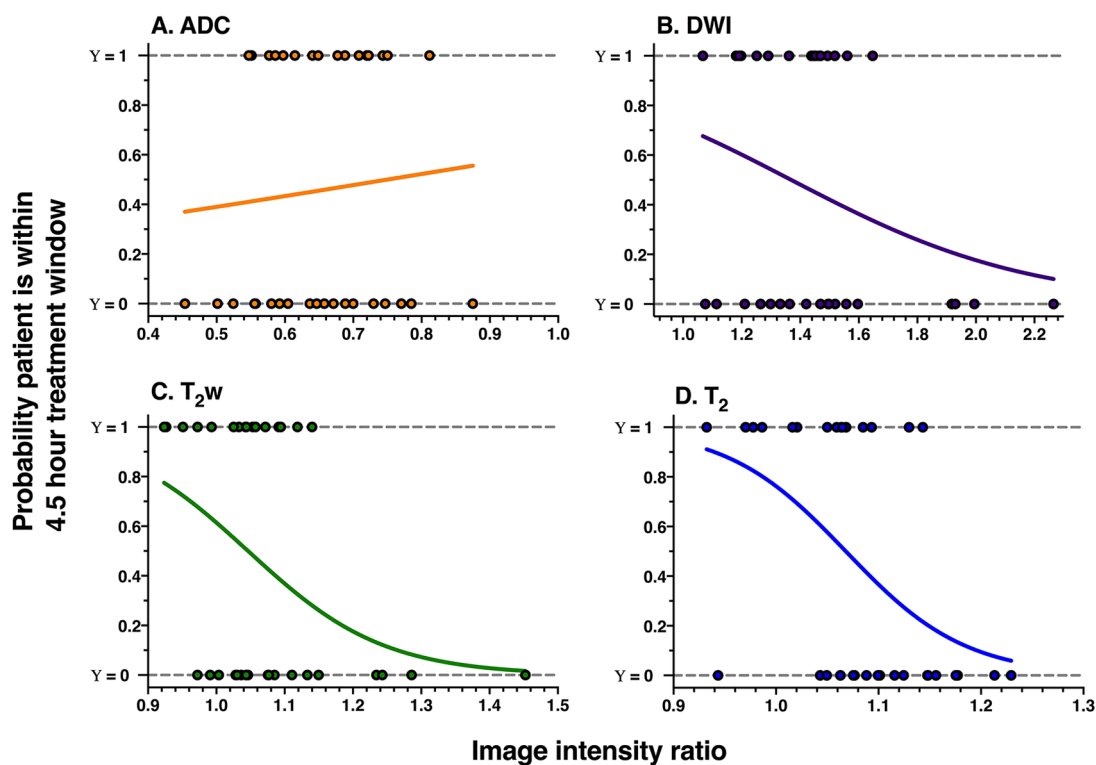

Figure 5. Probability plots for (A) ADC, (B) DWI, (C) T_2w, and (D) T_2 relaxation time image intensity ratios, derived from all 35 patients. The curves are the logistic fits that model the probability of a patient being within the 4.5-hour thrombolysis treatment window (y-axis) as a function of the image intensity ratio (x-axis). Dots represent image intensity ratios of individual patients who are within ($Y = 1$) or beyond ($Y = 0$) the treatment window. ADC indicates apparent diffusion coefficient; DWI, diffusion-weighted imaging.

sensitivity) but at the expense of falsely regarding many patients beyond the time window as within it (low specificity). With these optimal image intensity ratio cut-offs, PPVs were calculated for T_2 (70.59% CI: 51.79-84.28), ADC (50.0% CI: 45.15-54.85), DWI (59.09% CI: 45.97-71.03), and T_2w (57.14% CI: 43.43-69.84), and indicate that the T_2 ratio has the highest probability of correctly predicting whether a patient who is identified by this parameter as being within the

treatment window, is actually within the window. Except for ADC, where NPV = 100%, NPVs were comparable for DWI (76.92% CI = 52.46-86.6), T_2w (71.43% CI = 49.16-86.6), and T_2 (77.78% CI = 58.97-89.50). The performance of image intensity ratio cut-offs is further illustrated in Figure 2, which shows how patients were classified when cut-offs were applied.

Derived from logistic regressions, Figure 5 depicts that the probability that a patient is within the treatment window is

Table 3. Information for the logistic regression analysis.

MODEL	β (SE)	*T*-STATISTIC	*P*	OVERALL MODEL EVALUATION			
				χ^2	*DF*	*P*	AIC$_C$
ADC				0.24	33	.626	52.03
ADC ratio	1.79 (3.68)	0.49	.627	–	–	–	–
Intercept	−1.34 (2.43)	−0.55	.582	–	–	–	–
DWI				2.76	33	.097	49.50
DWI ratio	−2.44 (1.61)	−1.51	.130	–	–	–	–
Intercept	3.34 (2.33)	1.44	.150	–	–	–	–
T$_2$w	–	–	–	5.38	33	.020*	46.88
T$_2$w ratio	−10.05 (5.29)	−1.90	.057	–	–	–	–
Intercept	10.514 (5.58)	1.88	.060	–	–	–	–
T$_2$				8.41	33	.004*	43.85
T$_2$ ratio	−17.13 (7.09)	−2.42	.016*	–	–	–	–
Intercept	18.3 (7.64)	2.39	.017*	–	–	–	–
Combined				9.75	30	.045*	48.52
Intercept	22.05 (10.23)	2.15	.031*	–	–	–	–
ADC ratio	−0.07 (5.90)	−0.01	.990	–	–	–	–
DWI ratio	0.72 (3.52)	0.21	.837	–	–	–	–
T$_2$w ratio	−7.57 (8.78)	−0.86	.389	–	–	–	–
T$_2$ ratio	−14.05 (7.69)	−1.83	.068	–	–	–	–

Abbreviations: ADC, apparent diffusion coefficient; AICc, Akaike information criterion corrected for sample size; *df*, degrees of freedom, DWI, diffusion-weighted.
β is the estimated coefficient of the ratio or intercept, SE is the estimated standard error of β, *t*-statistic = β divided by the SE, *P* is the significance level.
*P < .05.

higher when the DWI, T$_2$w, and T$_2$ ratios are smaller and that the T$_2$ relaxation time ratio offers the highest probability (up to 90%). As the ADC values decrease during ischemia, higher ADC ratios indicate a higher probability of being within the treatment window. However, of those plots displayed in Figure 5, the results of the regressions indicate that only the T$_2$ relaxation time and the T$_2$w ratios were significant predictors of whether the patient was within the treatment window (Table 3). Table 3 also shows that the combined model involving all 4 image intensity ratios significantly predicted the probability of a patient being within the treatment window, but not to the same extent as the single-parameter regressions on the T$_2$w ratio and, in particular, the T$_2$ relaxation time ratio. Closer examination of the contribution of each parameter in the combined model (*P* values, Table 3) shows that the intercept was the only significant contributor to the model and that the T$_2$ ratio, although not significant, had the most dominant contribution (*P* = .068). Overall, the T$_2$ relaxation-time-ratio-only model was the best predictor of whether a patient is within or beyond the treatment window, as compared with other models, and it was the most significant and had the lowest AIC$_c$.

Subcohort with FLAIR MRI. The agreement between raters of the DWI/FLAIR mismatch was intermediate to good, with a free-marginal Fleiss kappa value of 0.59 (CI = 0.36-0.82), and 72.8% agreement.[35,36] All image intensity ratios did not correlate significantly with time from symptom onset (see SI Table 1 in supplementary materials), likely due to the small number of patients in the subcohort (Table 2). Figure 6 shows the PRG curves and associated AUPRGs. The AUPRGs were highest for the T$_2$ relaxation time ratio and DWI ratio, suggesting both parameters have good overall ability at identifying patients within the thrombolysis treatment window. However, the T$_2$ relaxation time curve was closest to the top right-hand corner of the graph, possibly suggesting a superior ability to the T$_2$w ratio. The AUPRGs were lowest for the T$_2$w and FLAIR ratios, demonstrating poor overall ability. Superior performance of T$_2$ relaxation compared with other parameters was also reflected by the F$_1$ score which was highest for the T$_2$ relaxation time ratio (0.73, CI = 0.52-0.94), lower for the ADC (0.59, CI = 0.35-0.82), DWI (0.67, CI = 0.44-0.89), T$_2$w (0.59, CI = 0.35-0.82), and FLAIR (0.57 CI = 0.34-0.81) ratios, and very low for the DWI/FLAIR mismatch (0.25, CI = 0.15-0.35).
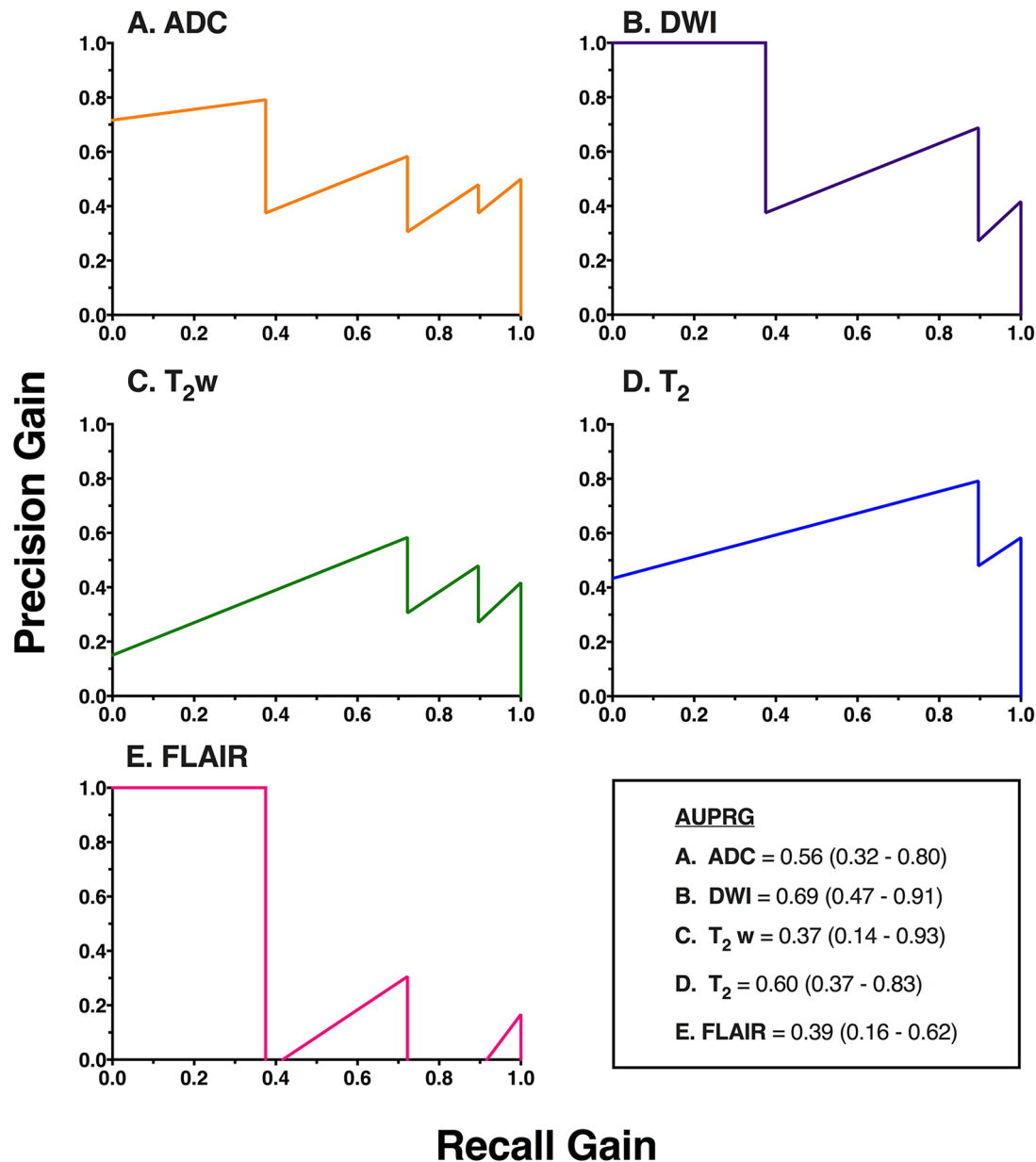
Figure 6. PRG curves and AUPRG curves from the subcohort of patients with additional FLAIR scans. The y-axis shows precision-gain, and the x-axis shows recall-gain values. Lines closest to the top right of the graph indicate parameters with high overall ability to identify patients scanned before 4.5 hours. An AUPRG of 0 indicates a trivial classifier, and positive and negative AUPRGs indicate more and less optimal classifiers, respectively. AUPRG values are given, with 95% confidence intervals in brackets. ADC, apparent diffusion coefficient; AUPRG, areas under the PRG; DWI, diffusion-weighted imaging; PRG, precision-recall-gain.

Discussion

In this study, the overall performance of quantitative and visual MRI-based methods for estimating stroke onset time, in the same cohort of hyperacute stroke patients, was compared. The T_2 relaxation time ratio outperformed ADC, DWI, T_2w, FLAIR image intensity ratios and the visual DWI/FLAIR mismatch, and combining ADC, DWI, T_2w and T_2 ratios showed no benefit. Results, therefore, suggest that the acquisition of T_2 relaxation times, with ADC for lesion localization, may be sufficient for estimating stroke onset time.

Our results support recent conclusions drawn from preclinical[14,25,47,48] and clinical[16,18] studies that the T_2

relaxation time detects brain ischemia and estimates onset time more accurately than MRI parameters derived from weighted images. Studies in rat models of ischemia reported strong relationships of the T_2 relaxation with time from stroke onset[14,15,47] and that onset time estimates made with T_2 had a lower margin of error than when intensities of weighted images were used.[25,47,48] The T_2 relaxation time also demonstrated higher overall ability at differentiating between scans performed before and after 3 hours from ischemia onset in rat models.[25]

Patient studies have shown the T_2 relaxation time to have a strong linear relationship with time from symptom onset[16-18]

and high overall ability at distinguishing between patients within and beyond the thrombolysis time window.[17,19] In this study, the AUC of the T_2 relaxation time ratio shows that 77% of the time, a randomly selected patient scanned within 4.5 hours of symptom onset had a lower T_2 than a randomly selected patient scanned at a time later than 4.5 hours. Similarly, previous patient studies have reported 76% using hemispheric differences in T_2 relaxation times at 1.5T for a 3-hour time window[17] and at 3T for a 4.5-hour time window, 71% using the T_2 change (difference), and 81% using a user-independent technique to quantify T_2 changes.[19]

The potential utility of FLAIR imaging for estimating onset time has received considerable attention within the stroke imaging literature (see Etherton et al[8] for review) but has only recently been directly compared with the T_2 relaxation time.[16] Results by Duchaussoy et al[16] and from our study suggest that the T_2 relaxation time will provide a more accurate estimation of stroke onset time than FLAIR-based approaches. Duchaussoy et al[16] reported a stronger relationship for T_2 relaxation with time from symptom onset compared with FLAIR image intensities (T_2: $r = 0.65$ vs FLAIR: $r = 0.18$) in a cohort of stroke patients scanned within 4.5 hours of symptom onset. We extended these findings by showing that the stronger relationship with time also applies when scans performed up to 9 hours from symptom onset are considered, all patients: $r = 0.49$ (T_2); subcohort: $r = 0.35$ (T_2), $r_s = 0.25$ (FLAIR). In further support, in the subcohort of patients with additional FLAIR scans, the T_2 relaxation time ratio demonstrated a much higher overall ability than the FLAIR ratio at identifying patients scanned within the thrombolysis treatment window. The ability of the FLAIR ratio and the DWI/FLAIR mismatch approach was comparatively weak, which is in accordance with previous studies that have reported low sensitivity of FLAIR-based methods.[8,49,50]

The changes in T_2 relaxation that occur during early ischemia reflect the radical changes in water dynamics caused by anoxic depolarization, whereby water is shifted from the extracellular to intracellular compartment, ie, cytotoxic edema, followed by the time-dependent breakdown of intracellular macromolecules.[51] The same pathophysiological factors (cytotoxic edema with the breakdown of intracellular macromolecules) that cause changes in T_2 relaxation, therefore, also contribute to the signal of images with a T_2w component. This contribution will explain why other patient studies[23,24,28] have reported a relationship for DWI and FLAIR image intensities with time from symptom onset. Despite the complexity of contributions to the measured T_2 relaxation time, being a single quantitative parameter, it is a more accurate measure of stroke onset time (and, possibly, of pathophysiological changes in ischemia) than image intensities from weighted images which are also influenced by other factors such as proton-density, T_1 relaxation, pulse sequence parameters, and inhomogeneities in B_0 and B_1. The increase in T_1 relaxation during ischemia would

decrease the T_2w and FLAIR signals in lesions unless the images are acquired with very long time of repetition (TR) ($>10\,000$ ms at 3T),[14] which may explain why T_2w and FLAIR ratios did not increase significantly in this study. Bias field problems may also be problematic in weighted images. The benefit of quantifying the T_2 relaxation time is that in computing the T_2 images, sources of error described above are removed. Thus, using T_2 relaxation instead of weighted images for stroke timing uses the dependence of T_2 on ischemia while removing confounding factors, making it a potentially more reliable stroke timer.

This study has some limitations that require consideration. First, it was a pilot study with a modestly sized unselected cohort of people with stroke symptoms, consisting of strokes of varying size and severity, that occurred in different vascular territories and tissue types. Recent results suggest the time dependency of T_2 during the first 9 hours of stroke does not differ between grey and white matter,[18] but it is currently unclear whether this is true for different vascular territories. A previous study[27] found lesion size to be a mediating factor in the relationship of DWI image intensity ratios with time from onset. It is, therefore, possible that the wide range of lesion sizes included in this study introduced some variability in the data, which could underlie the weak correlations of some of the parameters. Other clinical variables, which could not be accounted for in this study, may also affect the relationship of image intensity ratios over time. For example, collateral status has been shown to influence the relationship of FLAIR image intensities with time from symptom onset.[52]

Second, due to the clinical nature of the study, most MRI scans were acquired after thrombolysis was administered (74.3% all patients and 82.4% in subcohort), which is not representative of patients with an unknown onset time. Nevertheless, based on both preclinical[53] and clinical data,[18,54] we do not think that rtPA will have had a significant effect on the T_2 values within the lesion because the average ADC lesion values of the thrombolysed patients were not significantly different to the low ADC values of non-thrombolysed patients. Preclinical data suggest that if the ADC remains low following reperfusion, T_2 continues to increase with time.[53] In addition, a recent patient study[54] showed rtPA does not alter net water uptake in the ischemic lesion, and so by extension, T_2, which also reflects net water uptake, should not be altered. Furthermore, in our recent analysis of the patient cohort studied here, we found that the size of ADC lesions increased in 11 of 19 thrombolysed patients between initial (<9 hours onset) and follow-up scans (24+ hours), suggesting that ADC remained low long after rtPA, and thus rtPA would have had minimal or no effect on T_2 in the lesion.[18] However, to truly support this point, more information about blood flow would be needed, and a future study, including patients who undergo MRI before reperfusion therapies, is warranted. Regarding thrombolysis before MRI examination, it is well known in

clinical practice that rtPA administration may make the previously ischemic lesion DWI/ADC negative.[55] Potential normalization of DWI/ADC would not affect our analyses of the T_2 MRI signal characteristics, because only lesions with ischemic ADC were included.

Given the above limitations, further investigation in a larger patient cohort is required. Such a study would enable more FLAIR scans so that the FLAIR image intensity ratio and DWI/FLAIR mismatch can be compared fully with other parameters. Additional scans should be acquired that offer information on collateral status to determine the effects of thrombolysis, and whether it mediates the relationship of other MR parameters with time from onset. A more extensive study would also allow separation of data analysis into different vascular territories and lesion sizes and should involve validation of results in an unseen test data set.

In conclusion, this study suggests that the T_2 relaxation time may be the most accurate and reliable measure for estimating stroke onset time and that relying on weighted images as a method for stroke timing may be problematic. It also suggests that quantifying ADC for lesion identification and T_2 for onset time estimation will be sufficient, and other parameters are not needed. In terms of clinical practice and feasibility, quantifying ADC (for lesion localization) and T_2 relaxation times for onset time estimation requires minimal image processing. The MRI protocol adopted here is based on commonly available pulse sequences provided by all MRI vendors. Diffusion and multi-echo T_2 are quick and easy to acquire (~5 minutes maximum, in total, in this study), and most scanners automatically produce ADC and T_2 relaxation time images. With the advent of magnetic resonance fingerprinting[56] under-sampled image acquisition of both parameters could result in even shorter acquisition times, which is imperative in emergencies such as ischemic stroke where "time is brain."[57] The clinical feasibility of using magnetic resonance fingerprinting for assessment of hyperacute stroke patients has recently been demonstrated, where $2DT_1$ and FLAIR images and T_1 and T_2 relaxation time maps were acquired simultaneously within 4 minutes and 24 seconds.[16] The post-processing steps used in this paper were exploratory and not designed for a clinical setting. However fast and automatic delineation of ischemic regions on ADC images is already widely available,[58] and we have recently proposed a user-independent method for quantifying the impact of stroke on the human brain which has the potential to be easily automated for a clinical setting.[19]

Author Contributions

BLM contributed to study design, MRI analyses, data analysis, and writing the paper; RAD and MJK contributed to design of data analysis methods and statistics; IC contributed to MRI data analyses; GWJH, DC, PJ, AS, KWM, and PC contributed to patient recruitment and clinical assessment, and MRI scan acquisitions; RAK contributed to study design, oversight of the project, and paper writing.

ORCID iDs

Robin A Damion ![ORCID] https://orcid.org/0000-0003-2630-9914
Risto A Kauppinen ![ORCID] https://orcid.org/0000-0003-3383-6608

Supplemental Material

Supplemental material for this article is available online.

REFERENCES

1. Dekker L, Hund H, Lemmens R, Boiten J, van den Wijngaard I. Unknown onset ischemic strokes in patients last-seen-well >4.5 h: differences between wake-up and daytime-unwitnessed strokes. *Acta Neurol Belg.* 2017;117:637-642.
2. Thomalla G, Boutitie F, Fiebach JB, et al. Stroke with unknown time of symptom onset: baseline clinical and magnetic resonance imaging data of the first thousand patients in WAKE-UP (efficacy and safety of MRI-based thrombolysis in wake-up stroke: a randomized, doubleblind, placebo-controlled trial). *Stroke.* 2017;48:770-773.
3. Berkhemer OA, Fransen PSS, Beumer D, et al. A randomized trial of intraarterial treatment for acute ischemic stroke. *N Engl J Med.* 2015;372:11-20.
4. Nogueira RG, Jadhav AP, Haussen DC, et al. Thrombectomy 6 to 24 hours after stroke with a mismatch between deficit and infarct. *N Engl J Med.* 2018;378:11-21.
5. Powers WJ, Rabinstein AA, Ackerson T, et al. 2018 guidelines for the early management of patients with acute ischemic stroke: a guideline for healthcare professionals from the American Heart Association/American Stroke Association. *Stroke.* 2018;49:e46-e99.
6. Kauppinen RA. Multiparametric magnetic resonance imaging of acute experimental brain ischaemia. *Prog Nucl Magn Reson Spectrosc.* 2014;80:12-25.
7. Biggs D, Silverman ME, Chen F, Walsh B, Wynne P. How should we treat patients who wake up with a stroke? A review of recent advances in management of acute ischemic stroke. *Am J Emerg Med.* 2019;37:954-959.
8. Etherton MR, Barreto AD, Schwamm LH, Wu O. Neuroimaging paradigms to identify patients for reperfusion therapy in stroke of unknown onset. *Front Neurol.* 2018;9:327.
9. Busza AL, Allen KL, King MD, van Bruggen N, Williams SR, Gadian DG. Diffusion-weighted imaging studies of cerebral ischemia in gerbils. Potential relevance to energy failure. *Stroke.* 1992;23:1602-1612.
10. Gröhn OHJ, Kettunen MI, Mäkelä HI, et al. Early detection of irreversible cerebral ischemia in the rat using dispersion of the magnetic resonance imaging relaxation time, $T_{1}\rho$. *J Cereb Blood Flow Metab.* 2000;20:1457-1466.
11. Fiehler J, Foth M, Kucinski T, et al. Severe ADC decreases do not predict irreversible tissue damage in humans. *Stroke J Cereb Circ.* 2002;33:79-86.
12. Burgess RE, Kidwell CS. Use of MRI in the assessment of patients with stroke. *Curr Neurol Neurosci Rep.* 2011;11:28-34.
13. Schlaug G, Siewert B, Benfield A, Edelman RR, Warach S. Time course of the apparent diffusion coefficient (ADC) abnormality in human stroke. *Neurology.* 1997;49:113-119.
14. McGarry BL, Rogers HJ, Knight MJ, et al. Stroke onset time estimation from multispectral quantitative magnetic resonance imaging in a rat model of focal permanent cerebral ischemia. *Int J Stroke.* 2016;11:677-682.
15. Jokivarsi KT, Hiltunen Y, Gröhn H, Tuunanen P, Gröhn OH, Kauppinen RA. Estimation of the onset time of cerebral ischemia using $T_{1}\rho$ and T_2 MRI in rats. *Stroke.* 2010;41:2335-2340.
16. Duchaussoy T, Budzik J-F, Norberciak L, Colas L, Pasquini M, Verclytte S. Synthetic T_2 mapping is correlated with time from stroke onset: a future tool in wake-up stroke management? *Eur Radiol.* 2019;29:7019-7026.
17. Siemonsen S, Mouridsen K, Holst B, et al. Quantitative T_2 values predict time from symptom onset in acute stroke patients. *Stroke.* 2009;40:1612-1616.
18. Damion RA, Knight MJ, McGarry BL, et al. Quantifying T_2 relaxation time changes within lesions defined by apparent diffusion coefficient in grey and white matter in acute stroke patients. *Phys Med Biol.* 2019;64:095016.
19. Knight MJ, Damion RA, McGarry BL, et al. Determining T_2 relaxation time and stroke onset relationship in ischaemic stroke within apparent diffusion coefficient-defined lesions. A user-independent method for quantifying the impact of stroke in the human brain. *Biomed Spectrosc Imaging.* 2019;8:11-28.
20. Thomalla G, Cheng B, Ebinger M, et al. DWI-FLAIR mismatch for the identification of patients with acute ischaemic stroke within 4·5 h of symptom onset (PRE-FLAIR): a multicentre observational study. *Lancet Neurol.* 2011;10:978-986.
21. Aoki J, Kimura K, Iguchi Y, Shibazaki K, Sakai K, Iwanaga T. FLAIR can estimate the onset time in acute ischemic stroke patients. *J Neurol Sci.* 2010;293:39-44.
22. Petkova M, Rodrigo S, Lamy C, et al. MR imaging helps predict time from symptom onset in patients with acute stroke: implications for patients with unknown onset time. *Radiology.* 2010;257:782-792.

23. Cheng B, Brinkmann M, Forkert ND, et al. Quantitative measurements of relative fluid-attenuated inversion recovery (FLAIR) signal intensities in acute stroke for the prediction of time from symptom onset. *J Cereb Blood Flow Metab*. 2013;33:76-84.

24. Song SS, Latour LL, Ritter CH, et al. A pragmatic approach using magnetic resonance imaging to treat ischemic strokes of unknown onset time in a thrombolytic trial. *Stroke*. 2012;43:2331-2335.

25. McGarry BL, Rogers HJ, Knight MJ, Jokivarsi KT, Gröhn OHJ, Kauppinen RA. Determining stroke onset time using quantitative MRI: high accuracy, sensitivity and specificity obtained from magnetic resonance relaxation times. *Cerebrovasc Dis Extra*. 2016;6:60-65.

26. Xu X, Cheng Q, Zu Q, et al. Comparative study of the relative signal intensity on DWI, FLAIR, and T_2 images in identifying the onset time of stroke in an embolic canine model. *Neurol Sci*. 2014;35:1059-1065.

27. Madai VI, Wood CN, Galinovic I, et al. Clinical-radiological parameters improve the prediction of the thrombolysis time window by both MRI signal intensities and DWI-FLAIR Mismatch. *Cerebrovasc Dis*. 2016;42:57-65.

28. Wouters A, Cheng B, Christensen S, et al. Automated DWI analysis can identify patients within the thrombolysis time window of 4.5 hours. *Neurology*. 2018;90:e1570-e1577.

29. Thomalla G, Simonsen CZ, Boutitie F, et al. MRI-guided thrombolysis for stroke with unknown time of onset. *N Engl J Med*. 2018;379:611-622.

30. Bamford J, Sandercock P, Dennis M, Warlow C, Burn J. Classification and natural history of clinically identifiable subtypes of cerebral infarction. *Lancet*. 1991;337:1521-1526.

31. Zhang Y, Brady M, Smith S. Segmentation of brain MR images through a hidden Markov random field model and the expectation-maximization algorithm. *IEEE Trans Med Imaging*. 2001;20:45-57.

32. Smith SM. Fast robust automated brain extraction. *Hum Brain Mapp*. 2002;17:143-155.

33. Jenkinson M, Smith S. A global optimisation method for robust affine registration of brain images. *Med Image Anal*. 2001;5:143-156.

34. Shapiro SS, Wilk MB. An analysis of variance test for normality (complete samples). *Biometrika*. 1965;52:591-611.

35. Randolph JJ. Free-marginal multirater kappa (multirater K[free]): an alternative to Fleiss' fixed-marginal multirater kappa. Paper presented at: Joensuu Learning Instruction Symposium, Joensuu, Finland, 2005. https://eric.ed.gov/?id=ED490661. Accessed March 20, 2019.

36. Randolph JJ. Online kappa calculator. http://justusrandolph.net/kappa/. Published 2008. Accessed March 20, 2019

37. DeLong ER, DeLong DM, Clarke-Pearson DL. Comparing the areas under two or more correlated receiver operating characteristic curves: a nonparametric approach. *Biometrics*. 1988;44:837-845.

38. Youden WJ. Index for rating diagnostic tests. *Cancer*. 1950;3:32-35.

39. Symonds MRE, Moussalli A. A brief guide to model selection, multimodel inference and model averaging in behavioural ecology using Akaike's information criterion. *Behav Ecol Sociobiol*. 2011;65:13-21.

40. Berrar D, Flach P. Caveats and pitfalls of ROC analysis in clinical microarray research (and how to avoid them). *Brief Bioinform*. 2012;13:83-97.

41. Davis J, Goadrich M. The relationship between precision-recall and ROC curves. In: *Proceedings of the 23rd International Conference on Machine Learning – ICML '06*. Pittsburgh, PA: ACM Press; 2006:233-240.

42. Flach P, Kull M. Precision-recall-gain curves: PR analysis done right. In: Cortes C, Lawrence ND, Lee DD, Sugiyama M, Garnett R, eds. *Advances in Neural Information Processing Systems 28*. Red Hook, NY: Curran Associates, Inc; 2015:838-846.

43. Ozenne B, Subtil F, Maucort-Boulch D. The precision–recall curve overcame the optimism of the receiver operating characteristic curve in rare diseases. *J Clin Epidemiol*. 2015;68:855-859.

44. Rijsbergen CJV. *Information Retrieval*. 2nd ed. Newton, MA: Butterworth-Heinemann; 1979.

45. Bekkar M, Djemaa DHK. Evaluation measures for models assessment over imbalanced data sets. *J Inf Eng Appl*. 2013;3:27-38.

46. Sener RN. Diffusion MRI: apparent diffusion coefficient (ADC) values in the normal brain and a classification of brain disorders based on ADC values. *Comput Med Imaging Graph*. 2001;25:299-326.

47. Rogers HJ, McGarry BL, Knight MJ, Jokivarsi KT, Gröhn OHJ, Kauppinen RA. Timing the ischaemic stroke by 1H-MRI: improved accuracy using absolute relaxation times over signal intensities. *Neuroreport*. 2014;25:1180-1185.

48. Norton TJT, Pereyra M, Knight MJ, et al. Stroke onset time determination using MRI relaxation times without non-ischaemic reference in a rat stroke model. *Biomed Spectrosc Imaging*. 2017;6:25-35.

49. Wouters A, Lemmens R, Dupont P, Thijs V. Wake-up stroke and stroke of unknown onset: a critical review. *Front Neurol*. 2014;5:153.

50. Ebinger M, Galinovic I, Rozanski M, Brunecker P, Endres M, Fiebach JB. Fluid-attenuated inversion recovery evolution within 12 hours from stroke onset a reliable tissue clock? *Stroke*. 2010;41:250-255.

51. Knight MJ, McGarry BL, Rogers HJ, Jokivarsi KT, Gröhn OHJ, Kauppinen RA. A spatiotemporal theory for MRI T_2 relaxation time and apparent diffusion coefficient in the brain during acute ischaemia: application and validation in a rat acute stroke model. *J Cereb Blood Flow Metab*. 2016;36:1232-1243.

52. Wouters A, Dupont P, Christensen S, et al. Association between time from stroke onset and fluid-attenuated inversion recovery lesion intensity is modified by status of collateral circulation. *Stroke*. 2016;47:1018-1022.

53. Kettunen MI, Gröhn OHJ, Lukkarinen JA, Vainio P, Silvennoinen MJ, Kauppinen RA. Interrelations of T_1 and diffusion of water in acute cerebral ischemia of the rat. *Magn Reson Med*. 2000;44:833-839.

54. Broocks G, Kniep H, Kemmling A, et al. Effect of intravenous alteplase on ischemic lesion water homeostasis. *Eur J Neurol*. 2020;27:376-383.

55. Nagaraja N, Forder JR, Warach S, Merino JG. Reversible diffusion-weighted imaging lesions in acute ischemic stroke: a systematic review. *Neurology*. 2020;94:571-587.

56. Ma D, Gulani V, Seiberlich N, et al. Magnetic resonance fingerprinting. *Nature*. 2013;495:187-192.

57. Saver JL. Time is brain – quantified. *Stroke*. 2006;37:263-266.

58. Straka M, Albers GW, Bammer R. Real-time diffusion-perfusion mismatch analysis in acute stroke. *J Magn Reson Imaging*. 2010;32:1024-1037.